

# Research on the Spatial and Temporal Evolution of Carbon Emission Intensity in China and its Influencing Factors from 2011 to 2020

Shaoxiong Wu<sup>1,\*</sup>, Zheng Wei<sup>2</sup>

<sup>1</sup>School of Mathematics and Statistics, Xiamen Institute of Technology, Xiamen, Fujian, 361024, China

<sup>2</sup>College of Sciences, Northeastern University, Shenyang, Liaoning, 110004, China

\*Corresponding author

**Abstract:** Based on the data of China's provincial carbon emissions and provincial GDP from 2011 to 2019, the carbon emission intensity (t/w Chinese yuan) is calculated, a descriptive analysis of China's provincial carbon emission intensity is conducted to demonstrate its spatial and temporal distribution, and the spatial autocorrelation analysis and geographic detector methods are used to quantitatively analyze the spatial and temporal variation characteristics of China's provincial carbon emission intensity from 2011 to 2019. The spatial autocorrelation analysis and the geodetector method are used to quantify the spatial and temporal characteristics of China's provincial carbon emissions intensity from 2011 to 2019. Finally, the top nine factors with the greatest explanatory power selected by the geographic detector are used as input variables, and the GRNN neural network is used to forecast China's carbon emission intensity in 2020. The study shows that (1) China's provincial carbon emission intensity collated in a decreasing trend from 2011 to 2019, indicating the significant effect of environmental protection policy implementation in these years (2) the spatial agglomeration of China's provincial carbon emission intensity from 2011 to 2019 is obvious, with an expanding trend in both the H-H region and the L-L region, with H-H spreading from Northwest China to Northeast China and the L-L region expanding to surrounding cities, (3) There is a spatially heterogeneous pattern of inter-provincial carbon emission intensity in China from 2011 to 2019. (4) From 2011 to 2019, the factor with the greatest explanatory power for China's provincial carbon emission intensity is average temperature, followed by industrial output, topographic relief, and science and technology expenditure. (4) For the projection of China's inter-provincial carbon emission intensity in 2020, the trend of carbon emission intensity is greatly related to geographical differences, which indicates that inter-regional exchanges and cooperation have a facilitating effect on carbon reduction policies.

**Keywords:** carbon emissions intensity, spatial and temporal distribution, spatial autocorrelation, geodetectors, GRNN

## 1. Introduction

With the continuous socio-economic development and the massive use of fossil energy, leading to the intensification of global climate problems, low carbon development has become a worldwide consensus, and China is the world's largest emitter of carbon dioxide, therefore, China's carbon dioxide emissions are of concern to the world. Carbon intensity is the amount of carbon dioxide emissions per unit of GDP growth (in t/w GDP) and is one of the most important indicators of carbon emissions. In order to accelerate the reduction of carbon intensity and achieve carbon emission targets, only by finding out the influencing factors of carbon intensity and understanding the process of carbon intensity change, can we take scientific measures to reduce carbon intensity.

International scholars have analyzed the spatial and temporal characteristics of the factors influencing carbon emissions and the intensity of carbon emissions through various econometric models. Grazios et al<sup>[1]</sup>, showed that the amount of gas pollution generated by manufacturing industries in Europe is related to the technology adopted. Richard York et al<sup>[2]</sup> used the STIRPAT model to find that population size, affluence, urbanization, and industrialization have an impact on carbon emissions. Peer Rebecca et al<sup>[3]</sup> explored the relationship between electricity production and carbon emissions. Sharma Rajesh et al<sup>[4]</sup> empirically showed that stock market development, per capita income and trade expansion have a catalytic effect on carbon intensity in South Asian countries based on the CS-ARDL approach. Talukdar et al<sup>[5]</sup> conducted data collection for 44 developing countries and concluded that an

increase in the share of secondary sector is directly related to an increase in carbon intensity.

Chinese scholars have also conducted studies on carbon emissions. Li Qianwen et al<sup>[6]</sup> demonstrated the existence of spatial aggregation of carbon emissions in China. Li Jianbao et al<sup>[7]</sup> used a spatial econometric model to analyse the factors influencing per capita CO<sub>2</sub> emissions in China. Meng Xiaona et al<sup>[8]</sup> used an SDN model and a mediating effects model to find that industrial intelligence indirectly suppresses carbon intensity by promoting industrial structure optimization and industrial structure rationalization. Clarke-Sather<sup>[9]</sup> et al. found that the uneven distribution of carbon emissions in China was mainly caused by geographical factors based on the IPCC method.

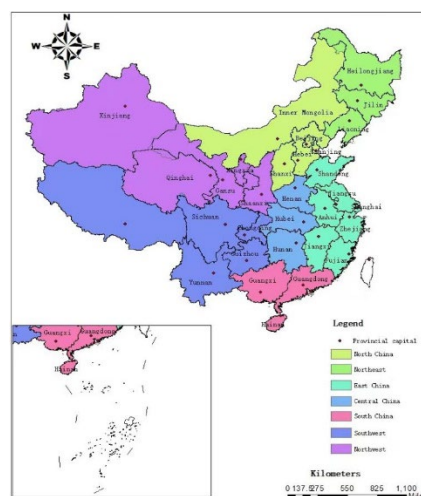
The factors influencing carbon intensity are directly related to the prediction of carbon intensity trends. There are many studies on carbon intensity prediction, such as using ELM model<sup>[10]</sup>, STRIPAT model<sup>[11,12]</sup>, IPAT<sup>[13,14]</sup>.

China uses carbon emission intensity as an indicator to formulate emission reduction policies<sup>[15]</sup>, but due to the large number and complexity of factors influencing carbon emission intensity, only a few simple driving factors were analysed in the above study, and the factors considered were rather homogeneous, which also led to the reduced stability and low accuracy of the prediction results of carbon emission intensity. In this paper, we analyse the spatial and temporal patterns and interannual variability of carbon emission intensity in China from 2011 to 2019 by mapping it with ARCGIS, and analyse the spatial correlation and local spatial correlation characteristics of carbon emission intensity by calculating Moran's I index and LISA clustering maps. A geographical probe was used to select 17 factors from four perspectives: socio-economic, climate, geographic environment and policy, to analyse the impact of carbon emissions intensity at the national scale. The top 9 factors with the greatest explanatory power were selected as input variables by the geographic detector, and a GRNN neural network was used to forecast the carbon emission intensity in 2020. The aim of this study is to provide a more scientifically sound and specific basis for decision-making on carbon emission reduction in China's provinces.

## 2. Materials and methods

### 2.1 Study area

China is located in the east of Asia and on the west coast of the Pacific Ocean. It has a vast and extensive territory with a total land area of approximately 9.6 million square kilometres, ranking 3rd in the world after Russia and Canada. China can be subdivided into seven major regions according to geographical location, namely North China, Northeast China, East China, Central China, South China, Southwest China and Northwest China. The study area for this paper is shown in Figure 1 and includes 30 mainland provincial cities in China, except for Hong Kong SAR, Macau SAR and Taiwan Province, and Tibet Autonomous Region.



Note: The plan has an examination number of GS (2020)4619 and the base plan has not been amended

Figure 1: A schematic diagram of the study area

## 2.2 Data sources

Based on the above literature and given the availability of data, 17 influencing factors were selected in the four dimensions of socio-economic, climate, geographical environment, and policy, using 30 Chinese provinces (urban areas) other than Tibet, Hong Kong, Macau and Taiwan as the study population ( $x_1 \sim x_{17}$ ). Carbon emissions data were obtained from the China Carbon Accounting Database (CEADs), spanning 2011 to 2019, and GDP data of each province were obtained from the China Statistical Yearbook, and carbon emissions intensity data from 2011 to 2019 were calculated by the carbon emissions intensity formula (carbon emissions/GDP) in (t/w Chinese yuan). gDp, total population ( $x_1$ ), GDP per capita ( $x_2$ ), amount of foreign investment ( $x_3$ ), the proportion of people employed in the secondary sector ( $x_4$ ), the proportion of employment in the tertiary sector ( $x_5$ ), investment in science and technology ( $x_6$ ), electricity consumption ( $x_8$ ), per capita consumption expenditure ( $x_9$ ) Data from the China Statistical Yearbook. Industrial output value ( $x_7$ ) Data from the China Industrial Statistics Yearbook. Average temperature ( $x_{11}$ ), average wind speed ( $x_{12}$ ) and precipitation ( $x_{10}$ ) Data from the National Center for Environmental Information (NCEI) under the National Oceanic and Atmospheric Administration (NOAA), green coverage of built-up areas ( $x_{14}$ ), industrial wastewater emissions ( $x_{15}$ ), industrial sulphur dioxide emissions ( $x_{16}$ ) Data from the China Environmental Statistics Yearbook. Search volume of environmental protection keywords ( $x_{17}$ ) are from the Baidu Index website. Topographic relief ( $x_{13}$ )<sup>[16]</sup> is a comprehensive representation of regional altitude and surface cut. Based on the definition of topographic relief and its calculation formulae in the context of habitat evaluation in China, the digital elevation model (SRTM 90 m) data were resampled into 1 km, and the model was used to calculate the terrain relief km grid dataset in China.

## 2.3 Research Methodology.

1) Spatial autocorrelation analysis: is a collection of spatial data analysis methods and techniques that can be applied to the study of carbon intensity to identify the degree of spatial agglomeration and dispersion of carbon emissions, which can be distinguished as global spatial autocorrelation, represented by the global Moran's I index, and local spatial autocorrelation, represented by the local Moran's I index, or by using the LISA aggregation diagram. There are five types of LISA clustering diagrams, regions with insignificant spatial correlation and four similar regions with significant spatial correlation. H-H is high-high clustering, L-L is low-low clustering, L-H is low-high clustering and H-L is high-low clustering.

2) Geographical detector: the carbon emission intensity of the 30 provinces in this study is taken as  $y$ . The factor detector in the geographical detector is used for the indicators obtained from the data collection from 2011 to 2019, and these indicators are taken as factor  $X$ . The extent to which factor  $X$  explains the spatial variation of the dependent variable  $y$  can be detected. The statistical value of  $q$  is commonly used to indicate that the value of  $q$  ranges from  $[0,1]$ , and the larger the value of  $q$ , the stronger the influencing factor is in explaining the carbon emission intensity.

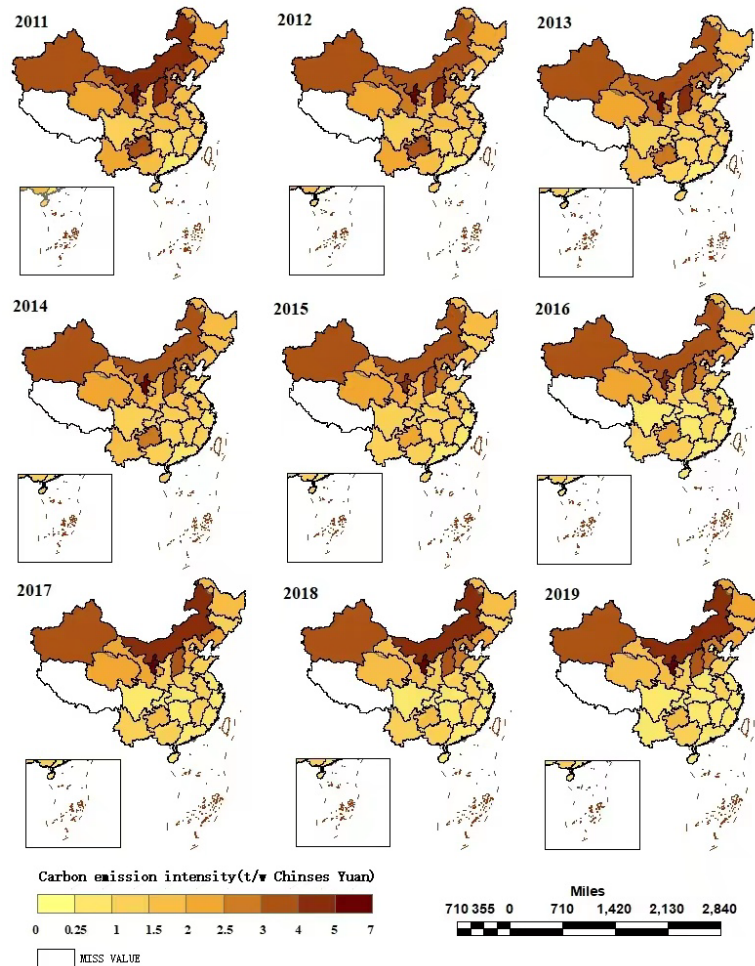
3) GRNN: A modification of RBF, the structure of both is similar. The difference lies in the addition of a summation layer and the removal of the connection between the implied layer and the weights of the output layer. The first layer is the input layer, which consists of the source nodes. The second layer is the pattern layer, where the number of neurons is equal to the number of samples learned. The third layer is the summation layer.

## 3. Results and analysis

### 3.1 Spatial and temporal patterns and interannual variation in carbon emissions intensity

The carbon emission intensity of China from 2011 to 2019 is divided into five levels: (low intensity) areas, which are set as carbon emission intensity less than or equal to 1 t/w; (medium and low intensity) areas, which are set as carbon emission intensity greater than 1 and less than or equal to 2; (medium intensity) areas, which are set as carbon emission intensity greater than 2 and less than or equal to 3; (medium and high intensity) areas, which are set as carbon emission intensity greater than 3 and less than or equal to 5; and (high intensity) areas, which are set as carbon emission intensity greater than or equal to 5. For (medium-intensity) areas, the carbon intensity is set to be greater than 3 and less than or equal to 5, and for (high-intensity) areas, the carbon intensity is set to be greater than 5, as shown in Figure 2.

(1) From 2011 to 2019, the spatial variation of carbon emission intensity of each province in China is obvious, East China, Central China and South China largely changed from medium-low intensity to low intensity, Northeast China except Jilin reduced from medium intensity to medium-low intensity, the remaining two provinces did not change significantly, Northwest China except Xinjiang and Ningxia the rest of the provinces changed from medium, medium-low intensity to medium-low intensity and low intensity, North China carbon emission intensity declined steadily, Beijing and Tianjin provinces dropped to low intensity. In 2011, there were only two provinces and cities in the low-intensity region, and six provinces and cities in the medium-intensity and above region; in 2019, there will be 14 provinces and cities in the low-intensity region, and only four provinces and cities in the medium-intensity and above region. Provinces and municipalities.



Note: The plan has an examination number of GS (2020)4619 and the base plan has not been amended

Figure 2: Changes in carbon intensity in 30 provinces and cities from 2011 to 2019.

### 3.2 Global spatial autocorrelation analysis of carbon emission intensity

Figure 3 shows the global autocorrelation Moran's I index of China's carbon emission intensity from 2011 to 2019. At the 1% significance level, the Moran's I index values for these nine years are all greater than zero, ranging from 0.29 ~ 0.397, which indicates that the carbon emission intensity of all Chinese provinces and cities show a positive correlation in these nine periods, with the overall Moran's I index from 2011 to 2019 Moran's I index fluctuates, but has an overall upward trend, peaking in 2019. It declines slightly during the period 2016-2018, but surges to a peak in 2019.

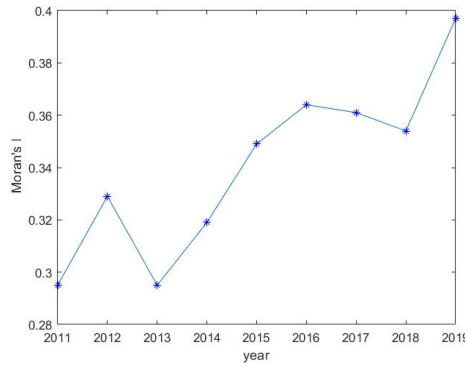
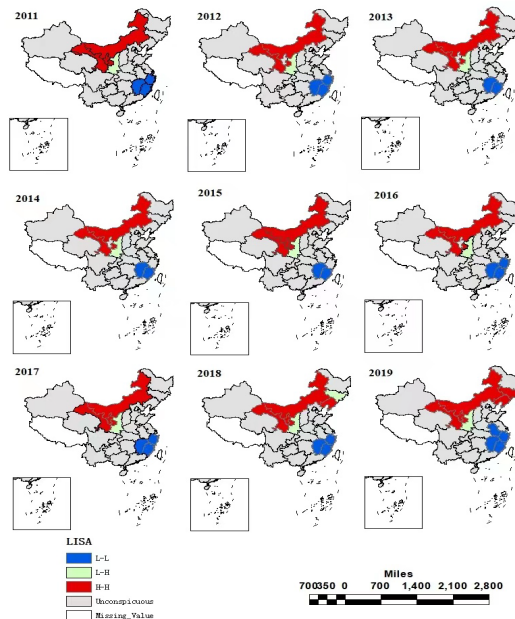


Figure 3: Moran's I changes in 30 provinces, 2011~2019

### 3.3 Local spatial autocorrelation analysis of carbon emission intensity

Figure 4 illustrates the spatial agglomeration characteristics of China's 30 provinces from 2011 to 2019, with H-H being high-high agglomeration, L-L being low-low agglomeration and L-H being low-high agglomeration, with provinces and cities with high carbon emission intensity and low carbon emission intensity in neighbouring regions generating relative agglomeration in space respectively.

(1) High-High Aggregation (H-H), in 2011, the H-H phenomenon appeared in Northwest, North China, and the range 2011-2019 showed an overall increasing trend, the carbon emission intensity in this region is greater than other regions, forming a spatial agglomeration of high carbon emissions. Ningxia has the H-H phenomenon in 2011, 2015, 2017-2019, and the rest of the years are not significant. This type of agglomeration spread from some adjacent areas in the northwest to some areas in the northeast from 2011-2019, and the provinces with high-high agglomeration were Gansu, Ningxia, Inner Mongolia, Jilin and Liaoning. (2) Low-low agglomeration (L-L), in 2011, Jiangxi, Fujian and Zhejiang provinces with low carbon emission intensity produced L-L phenomenon, from 2013 to 2015 this agglomeration area decreased, only two provinces in Fujian and Jiangxi, from 2016 to 2019 this agglomeration area increased, spread to the surrounding regions, reducing the carbon emission intensity of surrounding provinces and cities, in 2019, the H-H phenomenon increased to four provinces, respectively Jiangxi, Fujian and Zhejiang. Jiangxi, Fujian, Zhejiang and Anhui, respectively. (3) Low-high agglomeration (L-H), this type of region is less frequent and scattered, Shaanxi Province shows L-H phenomenon from 2011 to 2019. The distribution is around high carbon emission regions. 2018, Jilin Province showed L-H phenomenon, and then passed into H-H phenomenon in 2019.



Note: The plan has an examination number of GS (2020)4619 and the base plan has not been amended

Figure 4: Spatial clustering characteristics of carbon emission intensity from 2011 to 2019

### 3.4 Spatial heterogeneity analysis of carbon emission intensity

As shown in Figure 5, the spatial heterogeneity of China's provincial carbon emission intensity is shown by dividing the 30 provinces in this study into seven major regions, East China, North China, South China, Central China, Southwest China, Northwest China and Northeast China, with X in order 1~7, based on the geographic detector. According to the geodetector detection results, the q-values of spatial heterogeneity measures from 2011 to 2019 range from 0.329 to 0.439. q-values steadily increased from 2011 to 2016, reaching the maximum in 2016, indicating that the spatial heterogeneity is most obvious at this time. q-values fluctuated steadily from 2016 to 2019, reaching 0.423 in 2019. The q-values were all above 0.4 between 2014 and 2019.

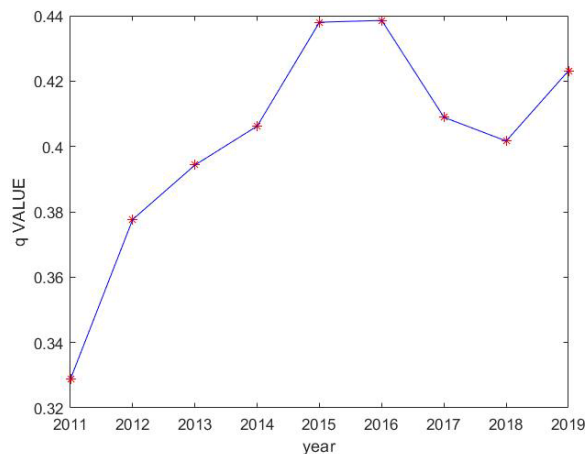


Figure 5: Spatial heterogeneity measure from 2011 to 2019

### 3.5 Analysis of factors influencing carbon emission intensity

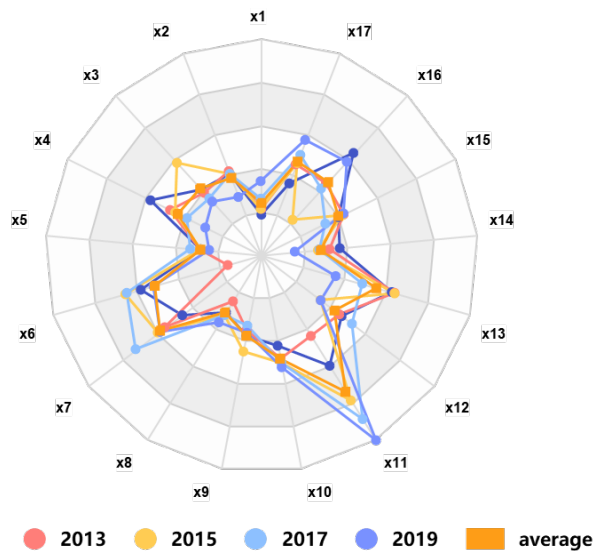


Figure 6: Radar chart of detection results of factors affecting national carbon emission intensity

In this paper, 17 factors were selected through four aspects: socio-economic, climate, geography and environment, and these 17 factors were divided into seven categories according to their numerical magnitudes through a hierarchical clustering method, and the degree of explanation of the spatial variation of carbon emission intensity by each factor was calculated through a factor detector. Due to the large span of years from 2011 to 2019, the survey was conducted in alternate years, and the five periods of 2011, 2013, 2015, 2017 and 2019 were investigated respectively. As shown by the q-values of each factor in Figure 6, it can be seen that the q-values of indicators such as topographic relief, the proportion of secondary industry and green cover show a decreasing trend, while the q-values of factors such as industrial output value, environmental protection keywords, precipitation and average

temperature show an increasing trend. From the average q-values of these five years, average temperature, industrial output value, terrain undulation degree, and science and technology expenditure have the greatest influence on carbon emission intensity. 2011 to 2019, the temperature difference between the northern and southern regions is obvious, with the south being warmer compared to the north, which leads to lower carbon emission intensity in the south than in the north. It became the main factor for the spatial divergence of carbon emission intensity between the south and the north. 2011~2019, the industrial output value of east China is much larger than that of northwest China, although high industrial output value will bring corresponding industrial pollution, but due to more advanced pollution control in east China and higher GDP from high industrial output value, the carbon emission intensity of east China is lower than that of northwest China. 2011~2019, the provinces and municipalities in Northwest and Northeast China both spent very little on science and technology, and the corresponding low-carbon technologies were not as good as those in other regions, so the carbon emission intensity in these two regions was high.

### 3.6 Analysis of GRNN prediction results

The top nine factors with the greatest explanatory power were obtained based on the average annual q-values of each factor obtained from the geographic probe, and these nine factors were used as input variables to the GRNN model, with the output layer being the carbon intensity.

The sample is nine indicators from 2011 to 2019, a total of 270 samples. Since the parameters have only one spread. So the optimal smooth coefficient spread was selected by getting the minimum RMSE one-dimensional, the optimal smooth coefficient spread=0.1 was obtained for prediction, and the test was carried out by the leave-one-out method, and the prediction result of the test was (RMSE = 0.33,  $R^2 = 0.9199$  ).

Therefore, under the smooth factor spread=0.1, all data from 2011 to 2019 were used as the training set to predict the carbon emission intensity in 2020. Table 1 shows the predicted data of 30 provinces and cities in 2020. Compared with the carbon emission intensity in 2019, the carbon emission intensity in East China, Central China, South China, Southwest China and Northwest China increases, except for Shandong and Ningxia provinces which are decreasing, among which Guizhou province increases the most, and the carbon emission intensity in North China and Northeast China decreases, except for Beijing which is increasing, among which Inner Mongolia decreases the most. This shows that the trend of carbon emission intensity is greatly related to geographical differences.

Table 1: Carbon intensity forecasts for 30 provinces and cities in 2020

Carbon intensity projections for 2020 (t/w Chinese yuan)					
Beijing	0.28004	Zhejiang	0.64221	Hainan	0.98723
Tianjing	0.90847	Anhui	1.45196	Chongqing	1.07939
Hebei	2.51308	Fujian	0.91073	Sichuan	1.23131
Shanxi	2.67162	Jiangxi	1.21293	Guizhou	2.61633
Inner Mongolia	3.59416	Shandong	1.03044	Yunnan	1.66773
Liaoning	1.99772	Henan	1.26806	Shaanxi	1.61370
Jilin	1.72312	Hubei	0.97292	Gansu	2.46737
Heilongjiang	1.84354	Hunan	1.14881	Qinghai	2.09868
Shanghai	0.62665	Guangdong	0.53423	Ningxia	5.44483
Jiangsu	0.91235	Guangxi	1.29367	Xinjiang	3.51138

## 4. Discussion

In this study, China's carbon emissions intensity from 2011 to 2019 is decomposed by provinces and cities, and it is found that Guizhou, Yunnan, Ningxia and Gansu provinces have higher carbon emissions intensity with larger changes, indicating that these provinces and cities have higher potential to reduce their carbon emissions intensity and need to take on more emission reduction targets. In contrast, Beijing, Shanghai, Fujian and Guangdong have lower carbon emissions intensity with smaller changes, indicating that these provinces have less potential to reduce carbon emissions and therefore do not need to take on more emission reduction targets.

As can be seen from the results in Figure 3, the global Moran's I index is positive over the period of this study, ranging from 0.29 ~ 0.397, and is generally on an upward trend. This indicates that the

spatial aggregation of provincial carbon intensity in China is becoming more and more evident, with neighbouring provinces and municipalities being mostly close to each other. The Lisa aggregation diagram reveals that the high carbon emission intensity agglomerations are located in parts of Northeast and North China, which geographically belong to the North. These provinces with high carbon emission intensity agglomerations have lower economic development and therefore have a greater potential for carbon emission decline, and with the exception of Liaoning, these regions' 2019 GDPs are in the middle and lower reaches of each Chinese province, so while strengthening environmental pollution in these cities. The two-pronged approach of strengthening environmental pollution control in these cities while also taking into account economic development will enable the carbon emission intensity of these provinces and cities to fall. The low carbon intensity catchment areas are located in the southern coastal provinces, which have a high level of economic development and are dominated by light industry, which puts less pressure on pollution control and therefore has less potential to reduce carbon emissions. Strengthening the exchange of economic and environmental pollution control policies between these regions is an important way to expand the low carbon emission intensity agglomerations and drive down the carbon emission intensity of surrounding cities.

According to the results of the analysis in Figure 5, Figure 6, the spatial heterogeneity generated by China's provincial carbon emissions intensity becomes more pronounced as the number of years increases, according to the seven regions of geographical location. This indicates that within the 30 provinces studied, China's provincial carbon emissions intensity shows a spatially heterogeneous pattern. At the national level, average mean temperature, industrial output, topographic relief and expenditure on science and technology have the greatest impact on carbon intensity, which is related to the difference in temperature between the north and south due to geographical location, and the national emphasis on vigorous industrial development and the improvement of science and technology.

The GRNN neural network used in this study used the top 9 factors with the strongest explanatory power as input variables for the prediction of carbon emission intensity, and cross-validation by the leave-one-out method illustrated good results for the prediction of carbon emission intensity.

## 5. Conclusion

(1) From 2011 to 2019, carbon emission intensity is on a downward trend, with low-intensity regions shifting from 2 provinces and cities to 14 provinces and cities, and medium-intensity regions shifting from 6 provinces and cities to 4 provinces and cities. The overall carbon emission intensity in East China, Central China and South China is smaller than that in Northwest China and Northeast China. (2) From 2011 to 2019, the carbon emission intensity of each region in China showed positive spatial correlation characteristics, and the carbon emission intensity pollution agglomeration from 2011 to 2019 was obvious, spreading from Northwest China to Northeast China. There is also agglomeration in low carbon emission intensity regions, with agglomeration areas in Jiangxi, Fujian and Zhejiang provinces spreading to the periphery and having the effect of reducing carbon emissions. There is an increasing trend in both the L-L region and the H-H region. (3) Through geographic detectors, at the national scale, the factor with the greatest explanatory power of carbon emission intensity in 30 Chinese provinces and cities is temperature, followed by industrial output value, topographic relief, and science and technology expenditure. 2011 to 2019, the spatial heterogeneity of carbon emission intensity shows an increasing trend. (4) The top nine most influential factors were obtained through the analysis of geographic detectors for GRNN neural network prediction, and the smooth coefficient spread was optimally selected using the leave-one-out method of cross-validation to obtain the 2020 carbon emission prediction data with the best prediction effect, and it can be found that the change trend of carbon emission intensity is greatly related to geographical differences.

## References

- [1] Francesco Graziosi, et al. Emissions of carbon tetrachloride from Europe [J]. *Atmospheric Chemistry and Physics*, 2016, 16(20): 12849-12859.
- [2] Richard York and Eugene A. Rosa and Thomas Dietz. A rift in modernity? Assessing the anthropogenic sources of global climate change with the STIRPAT model [International Journal of Sociology and Social Policy, 2003.] *International Journal of Sociology and Social Policy*, 2003, 23(10): 31-51.
- [3] Peer Rebecca A M and Chini Christopher M. Historical values of water and carbon intensity of global electricity production [J]. *Environmental Research: Infrastructure and Sustainability*, 2021, 1(2)

- [4] Sharma Rajesh et al. Examining the temporal impact of stock market development on carbon intensity: Evidence from South Asian countries. [J]. *Journal of environmental management*, 2021, 297: 113248-113248.
- [5] Debabrata Talukdar. Does the Private Sector Help or Hurt the Environment? Evidence from Carbon Dioxide Pollution in Developing Countries[J]. *World Development*, 2001, 29(5).
- [6] Li Qianwen, He Shan, Li Wanxing. Research on the factors influencing the carbon emission intensity of China's provincial areas[J]. *Journal of Wuhan University of Technology (Information and Management Engineering Edition)*, 2018, 40(03):295-299.
- [7] Li Jianbao, Zhang Zhiqiang, Qu Jiansheng, Xiong Yonglan. Analysis of spatial and temporal patterns of CO<sub>2</sub> emissions in Chinese provinces [J]. *Economic Geography*, 2014, 34(09):158-165.
- [8] Meng Xiaona and Xu Shichun and Zhang Jingnan. How does industrial intelligence affect carbon intensity in China? Empirical analysis based on Chinese provincial panel data[J]. *Journal of Cleaner Production*, 2022, 376
- [9] Afton Clarke-Sather, Jiansheng Qu, Qin Wang, Jingjing Zeng, Yan Li. Carbon inequality at the sub-national scale: A case study of provincial-level inequality in CO<sub>2</sub> emissions in China 1997-2007[J]. *Energy Policy*, 2011, 39(9).
- [10] Sun Wei and Huang Chenchen. Predictions of carbon emission intensity based on factor analysis and an improved extreme learning machine from the perspective of carbon emission efficiency [J]. *perspective of carbon emission efficiency*[J]. *Journal of Cleaner Production*, 2022, 338
- [11] Yang Fengmei, Shi Longyu, Gao Lijie. Probing CO<sub>2</sub> emission in Chengdu based on STRIPAT model and Tapio decoupling [J]. *Sustainable Cities and Society*, 2023, 89.
- [12] Zhao Y T , Huang X J , Zhong T Y , et al. Spatial Pattern Evolution of Carbon Emission Intensity from Energy Consumption in China[J]. *Environmental Science*, 2011.
- [13] Peng Fang. Short-term carbon emission prediction method of green building based on IPAT model [J]. *International Journal of Global Energy Issues*, 2023, 45(1).
- [14] Ozcan Burcu, Ulucak Recep. An empirical investigation of nuclear energy consumption and carbon dioxide (CO<sub>2</sub>) emission in India: Bridging IPAT and EKC hypotheses [J]. *Nuclear Engineering and Technology*, 2020, 53(6).
- [15] Hu Yuan, Liu Guichun, Kong Xiangzhen, Hu Wei. Analysis of spatial and temporal differences in carbon emission intensity in China [J]. *Resources and Industry*, 2016, 18(02): 67-75. DOI: 10.13776/j.cnki.Resources industries. 20160315.002.
- [16] You Zhen, Feng Zhiming\*, Yang Yanzhao. A kilometre grid dataset of topographic relief in China [DB/OL]. *Global Change Data Warehousing*, 2018. DOI:10.3974/geodb. 2018.03.16.V1